# Optimal Parameter Identification for Look-up Table based Band-limited Memory Polynomial Model using Direct and Indirect Learnings

Joel H. Chavez, Carolina L. R. Machado, Luis H. A. Lolis, and Eduardo G. Lima

Department of Electrical Engineering, Federal University of Paraná, Curitiba, Brazil
e-mail: elima@eletrica.ufpr.br

***Abstract*—The linearization of radio frequency power amplifiers (PAs) for wireless communication systems can be performed by a digital baseband predistorter (DPD). The DPD design includes the parameter identification of a post-inverse or a pre-inverse model. Such process depends on measurements of discrete-time complex-valued envelopes. With the adoption of larger envelope bandwidths and the PA operation at stronger nonlinear regimes, the requirements on the sampling frequency are very stringent. To relax the specifications on the analog-to-digital and digital-to-analog converters, a band-limited memory polynomial can be employed. To reduce the amount of calculations, polynomials can be replaced by linearly interpolated look-up tables (LUTs). Traditionally, a non optimal two step procedure is performed to identify the values to be stored in the LUTs. This work contribution is to propose an optimal identification technique that computes directly the values to be stored in the LUTs. The reported case study uses an LTE OFDMA envelope and Matlab simulation results show that the modeling accuracy can be significantly improved by the adoption of the proposed technique instead of the traditional one, quantified by reductions in normalized mean square error and adjacent channel power ratio of up to 10.8 dB and 12.4 dB, respectively.**

***Index Terms*—digital baseband predistortion; memory polynomial; power amplifier; radio frequency; wireless communication systems.**

## I. Introduction

Digital baseband predistorters (DPDs) are included in the transmitter chain of wireless communication systems for guaranteeing the required level of linearity, at the same time keeping the most power consuming element, which is the radio frequency (RF) power amplifier (PA), operating in an efficient way [1]. A common approach is to design the DPD block by using a discrete-time feed-forward dynamic nonlinear model with adjustable coefficients [2]. Examples include the Volterra series and its simplified versions like the memory polynomial (MP) [3].

Two DPD identification strategies are available [4]-[6]. The direct and indirect learning architectures are based on measurements of discrete-time complex-valued envelope signals. When an envelope signal passes through a nonlinear operator, its bandwidth is increased. A very high sampling frequency requires expensive and very power consuming analog-to-digital converters (ADCs) inside the measurement instruments [7]. For a given number of resolution bits, to relax the specifications on the instrument ADCs, in recent years some techniques were reported in literature for the identification of DPD schemes based on measurements adopting reduced sampling frequencies that comply with the Nyquist criterion only for the undistorted envelope signal [8]-[11]. The success of such DPD strategies using reduced sampling frequency, or equivalently under-sampling, is theoretically justified by the works of [12]-[14]. The work of [15] reports a comparison between the modeling accuracies of the direct and indirect learning architectures in scenarios of reduced sampling frequencies.

Digital-to-analog converters (DACs) are also necessary to feed the analog PA with a digitally predistorted signal whose bandwidth is wider than the undistorted one. In [16], a band-limited DPD was proposed to alleviate both ADC and DAC sampling frequency specifications. Such technique attenuates only the distortions located around the main channel and inside a bandwidth equal to the ADC and DAC sampling frequency.

In polynomial-based models, the amount of additions and multiplications required to process a single sample throughout the DPD model increases very rapidly with the polynomial order and memory depth. To relax the computational burden in real-time DPD application, in [17] polynomial functions are replaced by linearly interpolated look-up tables (LUTs). In such LUT-based models, the values to be stored in the LUTs become the adjustable coefficients. Traditionally, the parameter identification is performed in a two step procedure. First, the polynomial coefficients are found assuming the continuous model description. Then, the known polynomials are sampled at a finite number of amplitude levels to obtain the values to be stored in the LUTs. However, the optimality of the solution provided by the traditional approach can not be guaranteed. To circumvent such drawback and improve the modeling accuracy, this work proposes an identification technique that computes directly the values to be stored in the LUTs and, therefore, it is able to provide an optimum set of values.

This work is organized in the following manner. Section II addresses PA linearization through the use of DPDs. Direct and indirect learnings are detailed in Section III. Section IV describes the LUT-based band-limited MP model adopted in this work, whereas its parameter identification is discussed in Section V. Simulation results of a comparative study are reported in Section VI. Conclusions are provided in Section VII.

## II. Digital Baseband Predistortion

The block diagram of a DPD is shown in Fig. 1a. To co-

Digital Object Identifier 10.29292/jics.v13i2.36

rrect the nonlinearities introduced by the PA, a DPD block is put before the PA in a cascade connection. The DPD provides the inverse effect with respect to the behavior of the PA. Figure 1b shows three transfer characteristics: DPD transfer characteristic (DPD output $\tilde{v}_n$ as a function of DPD input $\tilde{x}_n$), PA transfer characteristic (PA output $\tilde{y}_n$ as a function of PA input $\tilde{v}_n$) and transfer characteristic of cascade connection between DPD and PA (PA output $\tilde{y}_n$ as a function of DPD input $\tilde{x}_n$). As illustrated in Fig. 1b, the DPD has an expansive characteristic, in contrast with the PA compression aspect. Besides, Fig. 1c indicates that the DPD is fed with an undistorted envelope $\tilde{x}_n$. Nonlinearities inside the DPD model intentionally distort the DPD output $\tilde{v}_n$, causing spectral regrowth in the signal applied as PA input. The nonlinear distortions generated by the PA cancel those produced by the DPD, providing an undistorted PA output $\tilde{y}_n$.

To design a DPD, a topology of its behavioral model must be selected. Such model must manipulate complex-valued envelopes, provide a nonlinear relationship between input and output envelopes, take into account memory effects and perform as few as possible computations. Neural networks and polynomials with memory are the most common choices [2]. In common, they have adjustable coefficients that must be chosen based on optimization procedures. In this work, polynomial approaches are employed because, in contrast to neural networks, they are linear in their parameters.

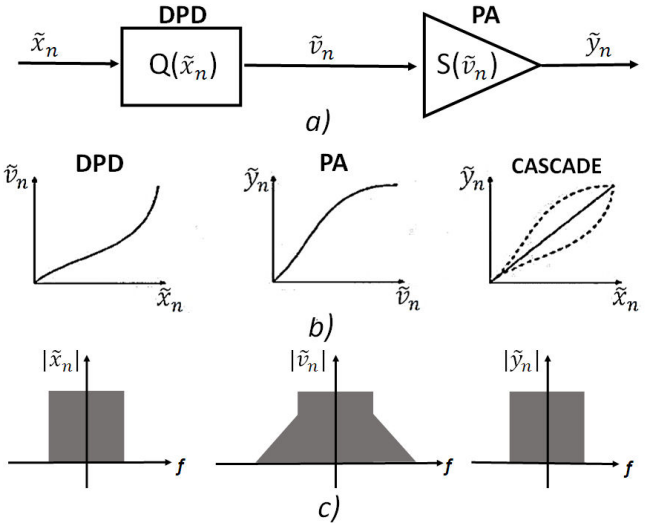


Fig.1 Basic concepts in DPD: a) block diagram of a cascade connection; b) transfer characteristic curves; c) power spectral densities.

## III. Direct and Indirect Learning Architectures

Once a DPD model is chosen, the next step is the identification of its parameters. This section addresses the direct and indirect approaches for performing such task.

### *A. Direct Learning*

Figure 2 shows the block diagram of the direct learning architecture [5]. Observe that the DPD desired output is not known. In a cascade connection of a DPD followed by a PA, the purpose is that the cascade output be a linear replica (apart from a linear gain *g*) of the cascade input. Hence, the DPD coefficient estimation by this method must include the PA model, which manipulates in a nonlinear way the DPD output. In this way, the coefficient extraction is posed as a nonlinear optimization problem, where the nonlinear function to be minimized is the mean square of an error signal $\tilde{e}_n$ defined by the difference between the DPD input signal $\tilde{x}_n$ and the PA output signal divided by *g* ( $\tilde{y}_n/g$).

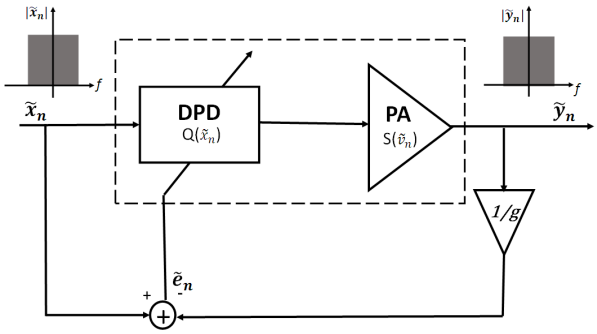


Fig.2 Direct learning architecture.

Therefore, direct learning, in addition to the need for a PA model, always requires nonlinear optimization algorithms, like Gauss-Newton, Levenberg-Marquardt [18]. Depending on the initial guess, such algorithms can be trapped in local minima that can only be corrected by the inclusion of additional algorithms (e.g. genetic algorithms, particle swarms, simulated annealing), which demand for greater computational complexity than a linear algorithm such as the least squares (LS). In the direct learning, the error signal has a bandwidth equal to the undistorted envelope signal.

### *B. Indirect Learning*

Indirect learning [6] is an architecture in which the coefficients of a post-distorter (PoD) – connected in cascade after a PA – is first identified and then copied to a DPD – connected in cascade before a PA – of same topology. In fact, for polynomial models truncated to the same order *P*, the pre- and post-inverse models are the same [19].

In a first PoD identification, as shown in Fig. 3a, the PA is excited by an undistorted input $\tilde{v}_n'$ and a distorted signal corrupted by spectral regrowth is measured at the PA output $\tilde{y}_n'$. Since the input and output roles are exchanged in PA and PoD blocks, the PoD input $\tilde{y}_n'/g$ is distorted (where *g* is the PA small-signal gain), while the PoD output $\tilde{w}_n$ is an undistorted signal. The polynomial parameters are obtained through a linear algorithm, such as LS, and then copied as parameters of a DPD of same topology. In a DPD, as shown in Fig. 1, the input $\tilde{x}_n$ is an undistorted signal and the output $\tilde{v}_n$ is a distorted signal. Hence, the DPD works in a differ-

ent configuration, concerning the input and output distortion levels, in comparison with the first identified PoD. As a consequence, degradation in linearization capability is expected. To solve this problem, the PoD parameter identification process must be repeated, but now with the PA excited by a predistorted signal obtained based on the DPD parameters previously identified, as shown in Fig. 3b. These new PA input $\tilde{v}_n''$ and output $\tilde{y}_n''$ signals are used to identify a second PoD, whose operation now resembles the operation of the DPD (e.g. undistorted input and distorted output). Novel PoD estimations can be computed, repeating the same procedure, but using the previous DPD as the starting point for collecting PA data. From the second PoD and so on, the error signal $\tilde{e}_n$ to be minimized is computed as the difference between two distorted signals.

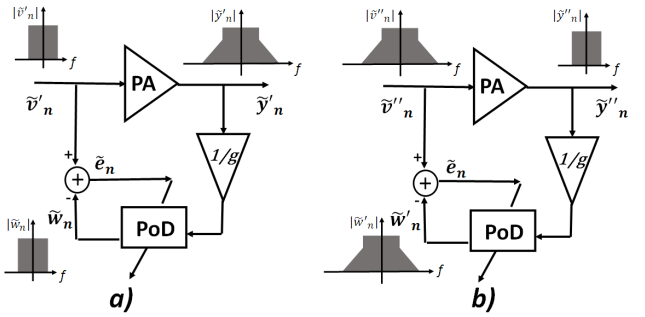


Fig.3 Indirect learning architecture: a) PoD first iteration; b) PoD second iteration.

## IV. LUT-BASED BAND-LIMITED MP MODEL

In this work, the DPD model is described by a band-limited MP model according to:

$$\tilde{v}_n = \left( \sum_{m=0}^{M} \tilde{x}_{n-m} \sum_{p=1}^{P} \tilde{h}_{m,p} a_{n-m}^{2(p-1)} \right) * \{LPF\}, \quad (1)$$

where $\tilde{x}_n$ and $\tilde{v}_n$ indicate complex-valued DPD input and output envelopes, respectively, $a_n$ is the amplitude component of $\tilde{x}_n$, $\tilde{h}_{m,p}$ are complex-valued parameters, $P$ is the polynomial order, $M$ is the memory length, * stands for convolution and $LPF$ refers to a lowpass filter. The block diagram of the band-limited MP model is shown in Fig. 4.

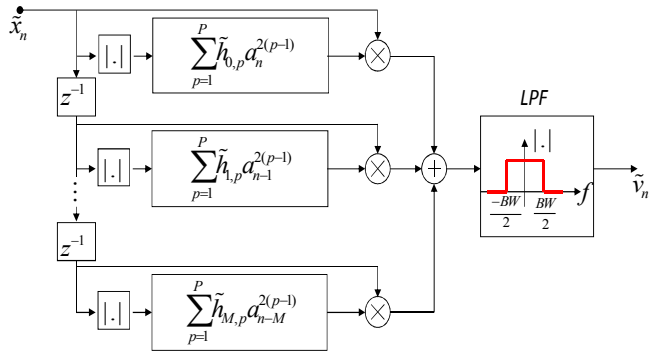


Fig.4 Block diagram of band-limited MP model.

As reported in [16], the lowpass filter has the purpose of constraining the spectral content of the predistorted signal inside the ADC/DAC sampling frequency of $BW$. Due to the limited bandwidth of (1), the DPD is only able to linearize the PA output at the frequency range from $-BW/2$ to $+BW/2$. For DPD purposes, the PA output must then be subject to a bandpass filter of same bandwidth.

The computation of outputs from polynomials such as (1) demands for a huge quantity of additions and multiplications. Besides, the amount of necessary calculation increases very rapidly with the polynomial order and memory length. As proposed in [17], to reduce the computational complexity the one-dimensional polynomials of (1) can be replaced by linearly interpolated look-up tables (LUT). To that purpose, first rewrites (1) as:

$$\tilde{v}_n = \left( \sum_{m=0}^{M} \tilde{x}_{n-m} f_m^{POL}(a_{n-m}^2) \right) * \{LPF\}, \quad (2)$$

where the one-dimensional polynomials $f_m^{POL}$ (for $m$ ranging from 0 to $M$) are given by:

$$f_m^{POL}(a_{n-m}^2) = \sum_{p=1}^{P} \tilde{h}_{m,p} a_{n-m}^{2(p-1)}. \quad (3)$$

Each $f_m^{POL}$ takes as argument a single real-valued information, given by the squared input amplitude component $a_{n-m}^2$. Each $f_m^{POL}$ returns a complex-valued information according to (3). Instead of performing all the additions and multiplications demanded by (3) at every time a new argument is applied, in the LUT-based approach each $f_m^{POL}$ is replaced by the storage of a finite number of $Q$ input and output values, as reported in Table I.

Table I. Information stored in a LUT with $Q$ addressable positions.

| LUT real-valued input | LUT complex-valued output |
|---|---|
| $e_{m,1}$ | $\tilde{s}_{m,1}$ |
| $e_{m,2}$ | $\tilde{s}_{m,2}$ |
| ⋮ | ⋮ |
| $e_{m,Q}$ | $\tilde{s}_{m,Q}$ |

In Table I, LUT real-valued inputs are designated by $e_{m,q}$ (with $q$ ranging from 1 to $Q$) and LUT complex-valued outputs are designated by $\tilde{s}_{m,q}$ (with $q$ ranging from 1 to $Q$). At every time a new argument $a_{n-m}^2$ is applied, the comparative operation $e_{m,q-1} \le a_{n-m}^2 \le e_{m,q}$ is performed to find the integer index $q$, which must be on the range from 2 to $Q$. The outputs $\tilde{s}_{m,q-1}$ and $\tilde{s}_{m,q}$ associated to the two consecutive LUT inputs $e_{m,q-1}$ and $e_{m,q}$ are read and, using linear interpolation, each $f_m^{POL}$ is approximated by:

$$f_m^{POL}(a_{n-m}^2) \approx \tilde{s}_{m,q-1} + \left( \frac{\tilde{s}_{m,q} - \tilde{s}_{m,q-1}}{e_{m,q} - e_{m,q-1}} \right) \left( a_{n-m}^2 - e_{m,q-1} \right). \quad (4)$$

The LUT-based technique allows for a simpler implementation because it reduces the amount of necessary additions and multiplications, at the expense of reading pre-

viously stored data and then performing linear interpolation. Indeed, in the LUT-based approach, according to (4), the computation of an output is always performed by the same number of additions and multiplications, independent of the polynomial order.

## V. Parameter Identification of the LUT-based Band-limited MP Model

This section addresses the identification of the band-limited LUT-based memory polynomial. Two techniques are reported here to find the LUT complex-valued output values $\tilde{s}_{m,q}$. All of the LUT real-valued input values $e_{m,q}$ are predetermined as equally spaced values starting in zero. The *LPF* and the values for *M*, *P* and *Q* are also assumed known before the $\tilde{s}_{m,q}$ parameter identification. First, a traditional technique based on a two step procedure is reported. Then, a proposed direct approach is introduced.

### *A. Traditional technique*

The traditional parameter identification method is divided into two processes. The first one is to calculate all of the polynomial parameters $\tilde{h}_{m,p}$ of (1). Because (1) is linear in the parameters $\tilde{h}_{m,p}$, such task can be performed by a linear method such as the LS. Given a set of *N* input and output data, all polynomial parameters can be found with:

$$\tilde{\mathbf{h}} = (\tilde{\mathbf{X}}_{POL}^{H}\tilde{\mathbf{X}}_{POL})^{-1}(\tilde{\mathbf{X}}_{POL}^{H}\tilde{\mathbf{v}}), \tag{5}$$

where the operator $(.)^H$ indicates the complex conjugate transpose, $\tilde{\mathbf{h}} = \begin{bmatrix}\tilde{h}_{0,1} & \cdots & \tilde{h}_{M,P}\end{bmatrix}^T$ is the row vector containing all the polynomial parameters, $\tilde{\mathbf{v}} = \begin{bmatrix}\tilde{v}_{1+M} & \cdots & \tilde{v}_N\end{bmatrix}^T$ is the row vector containing the output data and $\tilde{\mathbf{X}}_{POL}$ is the regression matrix which manipulates the input samples according to:

$$\tilde{\mathbf{X}}_{POL} = \begin{bmatrix} \tilde{x}_{1+M}a_{1+M}^{0} * LPF & \cdots & \tilde{x}_1 a_1^{2(P-1)} * LPF \\ \vdots & \vdots & \vdots \\ \tilde{x}_N a_N^{0} * LPF & \cdots & \tilde{x}_{N-M} a_{N-M}^{2(P-1)} * LPF \end{bmatrix}. \tag{6}$$

With all polynomial parameters identified, the second phase of this approach can be done, that is, all polynomial functions of (3) are evaluated having as argument each one of the LUT input values $e_{m,q}$ to provide the values for all $\tilde{s}_{m,q}$. Therefore, in the traditional approach, the order of the system to be solved by the LS is dependent on the polynomial order *P*, but not on the number of LUT addressable positions *Q*.

### *B. Proposed Technique*

The optimality of the solution provided by the LS in the traditional approach is assured only if continuous polynomial functions are employed. Hence, after the sampling of polynomial functions and the application of linear interpolation, there is no guarantee that the error is minimized. To circumvent such drawback of the traditional approach, this work proposes a technique that is able to provide an optimum set of values for the $\tilde{s}_{m,q}$ parameters. The proposed approach introduces a method to calculate all $\tilde{s}_{m,q}$ values directly, that is, without previously knowing any polynomial function. The band-limited LUT-based MP model is in fact also linear in the parameters $\tilde{s}_{m,q}$. As a consequence, the $\tilde{s}_{m,q}$ parameter identification can be performed into a single step by LS. Given a set of *N* input and output data, all $\tilde{s}_{m,q}$ can be found with:

$$\tilde{\mathbf{s}} = (\tilde{\mathbf{X}}_{LUT}^{H}\tilde{\mathbf{X}}_{LUT})^{-1}(\tilde{\mathbf{X}}_{LUT}^{H}\tilde{\mathbf{v}}), \tag{7}$$

where $\tilde{\mathbf{s}} = \begin{bmatrix}\tilde{s}_{0,1} & \cdots & \tilde{s}_{M,Q}\end{bmatrix}^T$ is the row vector containing all the LUT complex-valued parameters, $\tilde{\mathbf{v}} = \begin{bmatrix}\tilde{v}_{1+M} & \cdots & \tilde{v}_N\end{bmatrix}^T$ is the row vector containing the output data and $\tilde{\mathbf{X}}_{LUT}$ is the regression matrix which manipulates the input samples by:

$$\begin{bmatrix} \tilde{x}_{1+M}\mathbf{r}_0^{LUT}(a_{1+M}^2) * LPF & \cdots & \tilde{x}_1\mathbf{r}_M^{LUT}(a_1^2) * LPF \\ \vdots & \vdots & \vdots \\ \tilde{x}_N\mathbf{r}_0^{LUT}(a_N^2) * LPF & \cdots & \tilde{x}_{N-M}\mathbf{r}_M^{LUT}(a_{N-M}^2) * LPF \end{bmatrix}, \tag{8}$$

in which $\mathbf{r}_m^{LUT}(a_{n-m}^2)$ indicates column vectors with *Q* columns. The interpolated output of a given LUT depends only on the information of two consecutive positions of the given LUT. Hence, for each one of these $\mathbf{r}_m^{LUT}$, there are only two columns with non null values. In other words, any $\mathbf{r}_m^{LUT}$ is filled with (*Q*-2) null values. To obtain the two values different from zero to be inserted in each $\mathbf{r}_m^{LUT}$, first the integer index *q* between 2 and *Q* that satisfies $e_{m,q-1} \le a_{n-m}^2 \le e_{m,q}$ must be computed. Then:

$$\mathbf{r}_m^{LUT}(a_{n-m}^2) = [0 \quad \cdots \quad 0 \quad \tilde{r}_{m,q-1} \quad \tilde{r}_{m,q} \quad 0 \quad \cdots \quad 0], \tag{9}$$

$$\tilde{r}_{m,q-1} = 1 - \left[\frac{a_{n-m}^2 - e_{m,q-1}}{e_{m,q} - e_{m,q-1}}\right], \tag{10}$$

$$\tilde{r}_{m,q} = \left[\frac{a_{n-m}^2 - e_{m,q-1}}{e_{m,q} - e_{m,q-1}}\right]. \tag{11}$$

Therefore, in the proposed approach, the order of the system to be solved by the LS is dependent on *Q*, but not on the polynomial order *P*.

## VI. Validation

In this section, Matlab simulation results of several distinct DPDs are reported. The undistorted envelope signal is an LTE OFDMA with a bandwidth of 20 MHz. The PA to be linearized is described by (1), exchanging the input and output roles, with the complex-valued coefficients reported in Table II, followed by a lowpass filter with *BW* = 38.4 MHz described by an idealized frequency sequence of 4096 equally spaced samples, composed by ones and zeros for desired and undesired frequencies, respectively. The sampling frequency is set to 153.6 MHz. All the simulated DPDs share the LUT-based band-limited MP topology with $M = 1$, $Q = 4$, $e_{m,1} = 0$, $e_{m,2} = 1/3$, $e_{m,3} = 2/3$, $e_{m,4} = 1$ and using the aforementioned idealized frequency sequence to implement *LPF*. The DPDs differ among them by their

training algorithms. Both direct and indirect learning architectures, as well as traditional and proposed parameter identifications, are employed for the DPD identification. The traditional parameter identification approach assumes $P = 5$.

Table II. PA complex-valued coefficients.

| *Coeff* | *Value* | *Coeff* | *Value* |
|---|---|---|---|
| $\tilde{h}_{0,1}$ | -0.0515 - j0.0831 | $\tilde{h}_{1,1}$ | 1.0538 + j0.0612 |
| $\tilde{h}_{0,2}$ | 0.5407 + j0.0729 | $\tilde{h}_{1,2}$ | -1.6840 + j0.3680 |
| $\tilde{h}_{0,3}$ | -0.5777 + j0.0293 | $\tilde{h}_{1,3}$ | 2.9292 - j0.4123 |
| $\tilde{h}_{0,4}$ | 0.2852 - j0.1514 | $\tilde{h}_{1,4}$ | -3.2223 + j0.2051 |
| $\tilde{h}_{0,5}$ | -0.0218 + j0.1011 | $\tilde{h}_{1,5}$ | 1.3383 - j0.0130 |

The validation of the linearization capability of a DPD is assessed by the normalized mean square error (NMSE) [20] and the adjacent channel power ratio (ACPR). The ACPR calculation employs main channel bandwidth of 18 MHz, adjacent channels with 9 MHz bandwidth and frequency separation between main and adjacent channels of 14.7 MHz. Table III presents the results obtained with the distinct strategies.

Five iterations of the indirect learning architecture are reported in Table III. NMSE and ACPR values improved significantly from first to second iterations. These improvements reflect the behavior explained in Section III.B, since the second identified PoD works in a scenario closer to the DPD validation. Third to fifth iterations improve only slightly the linearization capability with respect to the second iterations. For the parameter identification with the direct learning architecture, Levenberg-Marquardt algorithm was used as the optimization algorithm by Matlab nonlinear least squares [18]. The initial guess uses the parameters found in the fifth iterations of indirect learning. In comparison with the indirect learning, the direct learning improves the NMSE and ACPR results up to 0.9 dB and 2.4 dB, respectively. However, such improvement can only be achieved at the expense of performing a nonlinear procedure.

Table III. NMSE and ACPR simulation results.

| | Traditional | | | Proposed | | |
|---|---|---|---|---|---|---|
| Architecture | Iter | NMSE [dB] | ACPR [dB] | Iter | NMSE [dB] | ACPR [dB] |
| Indirect Learning | 1st | -30.2 | -42.9 | 1st | -35.6 | -49.1 |
| | 2nd | -31.0 | -46.9 | 2nd | -40.0 | -52.8 |
| | 3rd | -31.1 | -47.0 | 3rd | -40.1 | -52.9 |
| | 4th | -31.1 | -47.0 | 4th | -40.1 | -52.9 |
| | 5th | -31.1 | -47.0 | 5th | -40.1 | -52.9 |
| Direct Learning | 18 | -31.5 | -47.5 | 15 | -41.0 | -55.3 |

In a comparison with the traditional technique, independent from the adopted learning architecture, the proposed technique always shows a superior behavior. In particular, improvements in NMSE results between 4.1 dB and 10.8 dB, as well as reductions in ACPR results between 1.6 dB and 12.4 dB, are reported when the proposed approach is employed instead of the traditional one. Figure 5 shows the power spectral densities (PSDs) of linearized PA output signals. A further substantial reduction in the distortions at adjacent channels is observed when the proposed technique is employed instead of the traditional one. Figure 6 shows the output amplitude as a function of the input amplitude for the PA model, the DPD model and the cascade connection of DPD followed by PA. Notice that the gain expansion of the DPD almost completely cancels the PA gain compression.

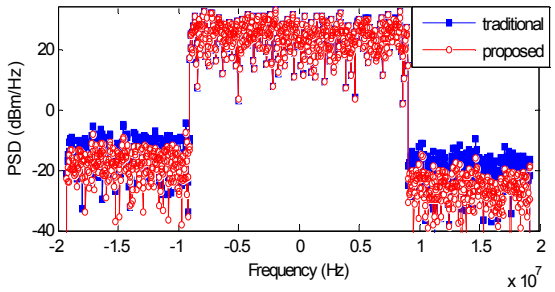


Fig.5 Power spectral densities (PSDs) of the linearized PA output signals, when the indirect learning with the traditional and proposed identification techniques is employed.

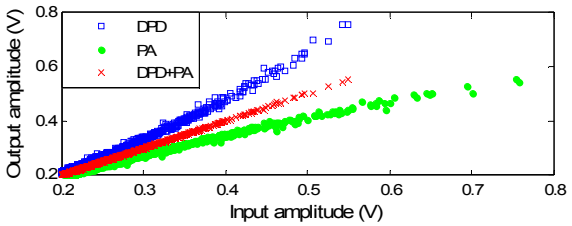


Fig.6 Transfer characteristics for: PA characteristic (in green color), DPD identified by indirect learning with proposed parameter identification (in blue color) and cascade connection of DPD followed by PA (in red color).

## VII. Conclusion

An optimal parameter identification for a band-limited LUT-based MP model is proposed in this work. Using two iterations of the indirect learning, which demands for the implementation of two least squares, NMSE and ACPR results of -40.0 dB and -52.8 dB, respectively, were obtained when the proposed technique is employed in the case study reported in this work. Conversely, the best NMSE and ACPR results obtained by the traditional approach, which was based on the direct learning that requires a nonlinear procedure, were equal to -31.5 dB and -47.5 dB, respectively. Therefore, a very significant superior performance is obtained by the proposed technique in comparison with the traditional one.

## Acknowledgements

The authors would like to acknowledge the financial

support provided by Coordenação de Aperfeiçoamento de Pessoal de Nível Superior and Organization of American States.

## REFERENCES

[1] P. B. Kenington, *High Linearity RF Amplifier Design*. Norwood, MA: Artech House, 2000.

[2] J. C. Pedro and S. A. Maas, "A comparative overview of microwave and wireless power-amplifier behavioral modeling approaches," *IEEE Trans. Microw. Theory Tech.*, vol. 53, no. 4, pp. 1150–1163, Apr. 2005.

[3] J. Kim and K. Konstantinou, "Digital predistortion of wideband signals based on power amplifier model with memory," *Electron. Lett.*, vol. 37, no. 23, pp. 1417–1418, Nov. 2001.

[4] R. N. Braithwaite, "General Principles and Design Overview of Digital Predistortion," in *Digital front-end in wireless communications and broadcasting circuits and signal processing*, Fa-Long Luo, Ed. Cambridge University Press, 2011, pp. 150–161.

[5] G. Baudoin and P. Jardin, "Adaptive polynomial pre-distortion for linearization of power amplifiers in wireless communications and WLAN," in *Proc. IEEE International Conference on Trends in Communications*, Bratislava, Slovakia, Jul. 2001, pp. 157–160.

[6] C. Eun and E. J. Powers, "A new volterra predistorter based on the indirect learning architecture," *IEEE Trans. Signal Process.*, vol. 45, no. 1, pp. 223–227, Jan. 1997.

[7] B. Murmann, "ADC Performance Survey 1997-2016," [Online]. Available: http://web.stanford.edu/~murmann/adcsurvey.html.

[8] Y. Liu, J. J. Yan, H. -T. Dabag, and P. M. Asbeck, "Novel Technique for Wideband Digital Predistortion of Power Amplifiers With an Under-Sampling ADC," *IEEE Trans. Microw. Theory Tech.*, vol. 62, no. 11, pp. 2604–2617, Nov. 2014.

[9] R. N. Braithwaite, "Closed-Loop Digital Predistortion (DPD) Using an Observation Path With Limited Bandwidth," *IEEE Trans. Microw. Theory Tech.*, vol. 63, no. 2, pp. 726–736, Feb. 2015.

[10] Y. Liu, W. Pan, S. Shao, and Y. Tang, "A General Digital Predistortion Architecture Using Constrained Feedback Bandwidth for Wideband Power Amplifiers," *IEEE Trans. Microw. Theory Tech.*, vol. 63, no. 5, pp. 1544–1555, May 2015.

[11] Q. Zhang, Y. Liu, J. Zhou, S. Jin, W. Chen, and S. Zhang, "A Band-Divided Memory Polynomial for Wideband Digital Predistortion With Limited Bandwidth Feedback," *IEEE Trans. Circuits Syst. II, Exp. Briefs*, vol. 62, no. 10, pp. 922–926, Oct. 2015.

[12] Y.-M. Zhu, "Generalized sampling theorem," *IEEE Trans. Circuits Syst. II*, vol. 39, no. 8, pp. 587–588, Aug. 1992.

[13] W. A. Frank, "Sampling requirements for Volterra system identification," *IEEE Signal Process. Lett.*, vol. 3, no. 9, pp. 266–268, Sep. 1996.

[14] J. Tsimbinos and K. Lever, "Input Nyquist sampling suffices to identify and compensate nonlinear systems," *IEEE Trans. Signal Process.*, vol. 46, no. 10, pp. 2833–2837, Oct. 1998.

[15] J. H. Chavez and E. G. Lima, "Direct and Indirect Learning for Predistorter Design Using Data with Reduced Sampling Frequency", in *Proceedings of the 32nd South Symposium on Microelectronics*, Rio Grande, May 2017, pp. 13–16.

[16] C. Yu, L. Guan, E. Zhu, and A. Zhu, "Band-Limited Volterra Series-Based Digital Predistortion for Wideband RF Power Amplifiers," *IEEE Trans. Microw. Theory Tech.*, vol. 60, no. 12, pp. 4198–4208, Dec. 2012.

[17] A. Kwan, F. M. Ghannouchi, O. Hammi, M. Helaoui, and M. R. Smith, "Look-up table based digital predistorter implementation for field programmable gate arrays using long-term evolution signals with 60 MHz bandwidth", *IET Sci. Meas. Technol.*, vol. 6, no. 3, 181–188, May 2012.

[18] J. Dennis Jr., "Nonlinear least-squares," in *State of the Art in Numerical Analysis: Conference Proceedings*, D. A. H. Jacobs, Ed. London: Academic Press, 1977, pp. 269–312.

[19] M. Schetzen, "Theory of pth-order inverses of nonlinear systems," *IEEE Trans. Circuits Syst.*, vol. 23, no. 5, pp. 285–291, May 1976.

[20] M. S. Muha, C. J. Clark, A. Moulthrop, and C. P. Silva, "Validation of power amplifier nonlinear block models," in *IEEE MTT-S Int. Microwave Symp. Dig.*, Anaheim, Jun. 1999, pp. 759–762.